10-18-95

SANDIA REPORT

SAND95–1556 • UC–410
Unlimited Release
Printed July 1995

Characteristics of the 2.65 μm Atomic Xenon Laser

Gregory A. Hebner

Prepared by
Sandia National Laboratories
Albuquerque, New Mexico 87185 and Livermore, California 94550
for the United States Department of Energy
under Contract DE-AC04-94AL85000

SF2900Q(8-81)

Issued by Sandia National Laboratories, operated for the United States Department of Energy by Sandia Corporation.

Available to DOE and DOE contractors from
Office of Scientific and Technical Information
PO Box 62
Oak Ridge, TN 37831

Prices available from (615) 576-8401, FTS 626-8401

Available to the public from
National Technical Information Service
US Department of Commerce
5285 Port Royal Rd
Springfield, VA 22161

NTIS price codes
Printed copy: A03
Microfiche copy: A01

SAND95-1556
Unlimited Release
Printed October, 1995

Distribution
Category UC-410

Characteristics of the 2.65 μm Atomic Xenon Laser

Gregory A. Hebner
Lasers, Optics and Remote Sensing Department
Sandia National Laboratories
Albuquerque NM 87185-1423

Abstract

The laser characteristics of the 2.65 μm atomic xenon laser transition are reviewed. Measured and extrapolated laser efficiency in nuclear pumped and electron beam pumped system is reported. Previous research has indicated that the reported power efficiency is between 0.1 and 2 percent.

Acknowledgments

The author thanks E. L. Patterson for sifting old data to identify the KITE cavity dimensions. The author further thanks P. J. Brannon, R. J. Lipinski and G. N. Hays for numerous helpful discussions. This work was performed at Sandia National Laboratories and supported by the United States Department of Energy under contract DE-AC04-94AL85000, the Arnold Engineering Development Center, Arnold Air Force Base, Tennessee, and by Princeton University.

Table of Contents

1. Introduction

Direct nuclear pumped lasers have been investigated for a number of years since they have the potential to be scaled to systems having long run times and high output powers.[1-25] One of the most extensively investigated systems is the atomic xenon laser which lases at numerous IR wavelengths between 1 and 4 μm, including 1.73, 2.03, 2.63, 2.65, 2.81 and 3.51 μm. Of these transitions, the 1.73 and 2.03 μm transitions have received the most amount of examination since they correspond to windows of good atmospheric transmission and have the highest reported efficiencies, 2.5 percent. Currently, there exists a good working knowledge of the important kinetic process and the influences of gas temperature, system design and gas mixture on the laser efficiency for these lines.

The purpose of this report is to review the available data, both generated at Sandia National Labs and elsewhere, on the 2.65 μm atomic xenon transition. This particular transition in atomic xenon has not been extensively investigated since the atmospheric transmission is relatively poor. However, the 2.65 μm transition lases very readily and appears in almost all studies using broad band cavity optics. In addition, it shares the same upper laser level as the 1.73 and 2.03 μm transitions (Fig 1). As a result, the experimental results[1-25] and models[26-29] that have been developed for the 1.73 and 2.03 μm transitions can potentially be extrapolated to the 2.65 μm transition (with due caution for the influance of the lower laser level).

One point to keep in mind when reviewing the data on atomic xenon is that the laser has transitions at 2.65 and 2.63 μm. In general, at low pump rates ($P <\sim 200$ W/cm^3), the 2.65 μm transition will dominate over the 2.63 μm transition due to much higher gain (as will be discussed

later).[25] As a result, unless care is exercised in identifying the laser output, it is possible to accidentally misidentify these two transitions.

In order to increase the amount of available data, this report begins with a discussion on the similarity of electron beam and nuclear excitation. Since fission-fragment excitation is similar to electron beam pumping, the results obtained by using electron beam pumping can be applied to questions associated with nuclear pumping. The available reactor and electron beam data will then be reviewed. The final result is a compilation of expected laser efficiency over a limited parameter space.

2.0 Comparison of nuclear and electron beam excitation

Due to the relative lack of data for the 2.65 μm atomic xenon transition using nuclear excitation, this report will include information obtained by electron beam excitation. However, before presenting that data, is important to examine the applicability of electron beam excitation as a simulation for nuclear excitation. Possible reasons for using electron beam pumping to simulate reactor pumping include the cost of the experiment, data rate and the generation of radioactive material. However, for applications requiring high output powers (Megawatts) and long pulse widths (0.1 s to CW), nuclear pumping is the technique of choice.

Nuclear excitation uses the kinetic energy of the fission products from ^{235}U, $^{3}He(n,p)^{3}H$, and $B^{10}(n,\alpha)Li^{7}$ reactions to produce ionization and excitation. For example, when ^{235}U in the form of a coating (typically UO_2) in contact with the gas mixture absorbs a thermal neutron, the nucleus fissions and produces energetic heavy nuclei with a combined energy of 160 MeV. A fraction of the fission products exit the coating and produce ionization and excitation in the laser gas mixture, primarily due to secondary electrons. Uranium fission-fragment excitation has an advantage over ^{3}He and ^{10}B excitation in that the higher energy of the fission-fragments (approximately 160 MeV total for ^{235}U fission- fragments as opposed to 0.75 MeV total for ^{3}He and 2.3 MeV for ^{10}B) can produce higher energy and power deposition, per cm^3, for similar gas mixtures.

Fission-fragment excitation offers several unique characteristics for investigating rare gas laser performance. The stopping range for fission-fragments at atmospheric pressure is shorter than the stopping range for 0.3 to 1.0 MeV electrons. For the case of one atmosphere of argon, the stopping distance for a 1 MeV electron is approximately three meters.[30] For helium, the

stopping distance for a 1 MeV electron in an atmosphere of helium is approximately 20 meters. In contrast, the stopping distance for an 80 MeV fission-fragment is approximately 10 cm in an atmosphere of helium and 3 cm in an atmosphere of argon.[29,31,32] As a result, the fission-fragments deposit a higher specific energy than an energetic electron beam in argon or helium.

2.1 Model predictions

Moratz, Saunders and Kushner compared the effects of heavy ion and electron beam excitation in both pure neon[32] and excimer laser mixtures.[29] In neon, the calculated secondary electron spectra produced by the slowing of a 1 MeV electron beam was compared with the result of ^{235}U fission fragment excitation. For this case, the secondary electron spectrum from the electron beam had a non-Maxwellian high energy tail and an electron temperature that was higher than the fission fragment excitation. The average energy of the secondary electrons from the electron beam was 150 eV as opposed to 40 eV for fission fragments. As a result, in an fission fragment pumped plasma, more of the input energy goes into excitation of lower energy levels as opposed to higher energy excitation and ionization.[32] As Moratz et al. point out, this is not necessarily bad, it all depends on the laser system and how the energy flows from the input into the desired transition.[32] However, in the atomic xenon system, the excited state transitions of interest are all less than 2 eV. Moratz et al. do not give any indication, in this work, how the secondary electron spectrums compare at these relativly low energies.

The codes developed to examine energy deposition in neon were expanded to examine the effects of pumping an excimer gas mixture.[29] For these calculations, the gas mixture was either $Ne/Xe/F_2$ or $Ne/Xe/NF_3$, mole fraction of 98.85/0.773/0.377, pressure of 1.36 atmospheres, and

peak energy deposition of 2.4 kW/cm^3. For these conditions, the electron beam pumped spectrum (1MeV electrons) extends beyond 2 keV while the fission fragment pumped spectrum barely exceeds 1 keV. However, for energies of approximately 3 to 20 eV, the electron energy distributions have nearly identical magnitudes and shapes. In addition, energy per ionization is approximately the same. While some of these results are gas dependent, there appears to be no significant difference between fission fragment and electron beam excitation.[29]

2.2 Experimental results

A series of experiments were performed at Sandia National Laboratories to compare atomic xenon laser operation with broadband mirrors using fission fragment excitation on the SPR-III reactor and long pulse electron beam excitation on the HAWK/KITE machine to resolve the issue of dominant output wavelength.[33] A question had been posed as to whether or not electron beam excitation was a valid simulation of fission fragment pumping due to possible differences in the electron density and average electron temperature. Previous experiments on SPR- III indicated that the dominant wavelength was 1.73 μm while the HAWK/KITE experiments showed the 2.63 or 2.65 μm transition was dominate. In the current experiments wavelength competition was investigated on SPR/KITE using the same cavity mirrors for both systems. Both SPR and KITE examined the laser characteristics using gas mixtures of Ar/Xe (0.995/0.005) at pressures of 5, 10, and 15 psia, and Ne/Ar/Xe (0.663/0.332/0.005) at 15 psia. The goals of this experiment were to evaluate whether fission fragment pumping and e-beam pumping are significantly different and to gain an insight into pertinent kinetic processes.

The back reflector for each cavity was a 5-m radius-of-curvature, overcoated silver, glass mirror. The reflectivity of this mirror is greater than 98% over the wavelength range from 1.73 to 3.51 μm. Two different output couplers were used. The first used a multilayer dielectric coating on infrared quartz and is referred to as "soft coatings" or the SPR-III mirror. The second was a HAWK/KITE mirror that was silver coated sapphire with an antireflection coating on the output side and have a reflectivity of 88% at 3.37 μm and 89% at 3.51 μm. The SPR-III and the HAWK/KITE output coupler reflectivity's at selected xenon laser wavelengths are shown in Table 1.

Table 1. Reflectivity of output couplers at selected wavelengths.

	Wavelength (μm)		
Output coupler	1.73 μm	2.03 μm	2.65 μm
Soft coating	88 %	96 %	67 %
Silver coating	76 %	80 %	84 %

The results of these experiments are shown in Figs. 2 and 3. The fission-fragment pumped results on SPR-III examined the wavelength distribution between 1.73 μm and 2.65 μm. Using the soft coating output coupler, gas mixtures of 5, 10 and 15 psia Ar/Xe and 15 psia, 2/1, Ne/Ar/Xe were examined. The silver, KITE output coupler was examined in 15 psia, 2/1, and Ne/Ar/Xe. Pump rates shown in the figures have been corrected for the underestimation of the input energy due to the rapidly cooled unpumped volume and the reactor pump power uncertainty is 20 %. The corrected energy is then normalized by the time dependent thermal neutron flux (derived from a cobalt based detector) to calculate an instantaneous pump power.[12-15]

Figures 2 and 3 show the comparison between the percentage of power in the 1.73 and 2.6 μm output for the HAWK/KITE experiments and the SPR-III experiments using the soft coatings. There is good agreement at all pressures on the relative fraction of 1.73 to 2.65 laser output. For these cavity conditions, the 1.73 μm line was dominant.

Comparison of Figs. 3a and 3b show the shift in dominant wavelength that occurs in both experiments as the output mirror reflectivity was changed. These results clearly indicate that the previous difference in wavelength between the KITE/HAWK data and the SPR-III data was due to differences in mirror sensitivity. The change in dominate output wavelength with relatively small changes in output coupler reflectivity suggests that the use of narrow band dielectric mirrors could eliminate laser output at all wavelengths beside the desired 2.65 μm. This point will be discussed later. In addition, comparison of the strong threshold behavior in Fig. 3 suggests that the pump rates are in good agreement. Because of the good comparison of the output wavelengths, there appears to be no significant differences between pumping with fission fragments or high energy electrons.

Thus the conclusion of both theoretical and experimental investigations is that there is no significant difference between electron beam and fission fragment excitation.

3.0 Review of nuclear pumped data

3.1 Review of 2.65 μm nuclear pumped laser

Nuclear pumped laser output at 2.65 μm has been measured from the very first reactor pumped atomic xenon experiments.[1] Early work noted that the laser output spectrum was a function of total pressure, buffer gas partial pressure, pump rate, gas temperature and cavity configuration.[1,3,5,9,10] However, the 2.65 μm transition has not been the subject of concentrated work due to its poor atmospheric transmission properties and the fact that the wavelength overlaps with the water absorption band in quartz. As a result, laser studies of this wavelength must use more exotic (and expensive) materials in order to avoid problems with intercavity absorption.

Nuclear pumped laser efficiency for the 2.65 μm transition has been reported by several Russian groups.[17,20] Melnikov and Sinyanskii have compiled a list of observed laser transitions, gas mixtures, pump rates and efficiencies.[20] The portion of that table that applies to the 2.65 μm transition is reproduced in Table 2. The highest measured efficiency was 1.5 percent for a 3 atmosphere gas mixture of He/Xe. The table also includes an efficiency of 2 percent for the 2.63 μm transition in Ar/Xe. This may very well be a misidentified transition.

Table 2. Results of Russian nuclear pumped laser research at 2.6 μm.[17,20]

Wavelength (μm)	Gas mixture	Pressure (atm.)	efficiency (%)	Pump power (W/cm^3)	reference
2.63	Ar/Xe	0.5	2.0	10.5	20
2.65	He/Xe	3	1.5	18	20
2.65	He/Xe	5	0.8	712	20
2.65	He/Ne/Xe	1.5	0.6	45	20
2.63	Kr/Xe	0.35	0.2	40	20
2.65	He/Xe	?	0.15	?	17
2.65 + 2.63	He/Ar/Xe	?	0.9	?	17

Magda reported an efficiency of 0.15 percent for a He/Xe gas mixture (2.65 μm) and 0.9 percent for a He/Ar/Xe gas mixture (2.63 and 2.65 μm).[17] Magda also presents results from both the Institute for Theoretical Physics (ITP, Magda) and the Institute for Experimental Physics (IEP, Melnikov and Sinyanskii[20]) and notes large differences in reported efficiencies. For example, the ITP measured a He/Xe efficiency of 0.15 percent while the IEP measured 1.0 percent.[17] He states that the discrepancy is due to the different methods used to measure the input power and the use of various correction factors to account for dimer radiation, gas motion, heat transfer to the cell walls, surface roughness of the ^{235}U layer and the ^{235}U composition.

Central to any calculation of laser efficiency is a determination of input power. However, one of the difficulties in nuclear pumped laser research is the accurate determination of input power. Energy deposition is usually determined in one of two ways. The first measures the pressure rise due to gas heating in the sealed laser chamber. The pressure rise is then corrected for gas mixture and geometry dependent heat transfer from the gas to the chamber walls to infer the peak energy deposition in the laser pump region. Typically, the energy input into the gas calculated from the ideal gas law is increased by a factor of 1.5 to account for the transfer of energy from the hot gas to the cool chamber walls.[14,15,17] The second method utilizes a measurement of the neutron flux and calculated coupling factors between the measured flux, thermal neutron flux, fission fragments produced in the ^{235}U layer, number of fission-fragments that exit the ^{235}U layer and heavy particle stopping in the gas. Both Magda and Sandia use the more direct pressure rise method and rely on established heat transfer codes for correction factors. Even if no correction factors are used, we (Sandia) over estimate the efficiency by a

factor of only 1.5. In the authors opinion, the accumulated errors in the neutron flux conversion can be much greater than 1.5. Thus, unless it is clearly stated how the input energy is derived, any laser efficiency number must be viewed cautiously.

3.2 General characteristics of the atomic xenon laser

The purpose of this section is to discuss some of the general characteristics of the nuclear pumped atomic xenon laser and review the important kinetics that influence the laser performance.

One of the issues associated with fission-fragment pumping is that the relatively high gas energy loadings routinely obtained using fission-fragment excitation (100's J/L) can produce gas temperature increases of several hundreds of degrees. Previous work suggested that gas temperature increases of this magnitude can detrimentally influence the laser gain and efficiency.[13-18] For example, the fission-fragment pumped 1.73 μm atomic xenon laser output can abruptly terminate before the peak of the pump pulse.[13,14] As a result, active gas cooling methods such as heat exchangers and flowing gas loops have been proposed and employed for high power laser systems to reduce the gas temperature to acceptable levels and achieve long run times.[2,19] However, heat exchangers and gas loops can increase the cost and complexity of a system. Since the complexity of the kinetics in these systems precludes detailed kinetic models, measurements are required of laser efficiency as a function to gas temperature to identify the optimum operating point that balances laser efficiency with system complexity.

Characteristics of the laser performance and possible origins of the abrupt turn off of the laser output has been illuminated by several detailed kinetic models.[26,27] Briefly, the upper energy

level of the atomic xenon laser is believed to be predominately populated by dissociative recombination of $ArXe^+$. An increase in the gas temperature reduces both the $ArXe^+$ association and dissociative recombination rates with a resulting increase in electron density. Reduced association and recombination rates decrease the rate of formation of the upper laser level. Increased electron density enhances electron collisional induced mixing of the laser manifold since the energy level spacing in the atomic xenon laser (5d and 6p levels) is relatively small. In addition, the laser manifold state to state quenching rates may also be temperature dependent due to heavy particle collisions.[34] Thus an elevated gas temperature negatively impacts several important laser processes.

In practice, the high energy loadings that result in elevated gas temperatures also produce high pump powers and electron densities. As a result, it has been difficult to deconvolve the kinetic effects due to electron collision induced mixing of the laser manifold at high pump powers from the multiple kinetic rate changes due to gas heating. Thus an experimental apparatus was recently designed to operate at low pump powers and energy loadings to reduce the electron density and fission-fragment produced gas temperature rises while externally controlling the gas temperature.[11] Measurements and calculations of the small signal gain at 1.73 and 2.03 μm in atomic xenon have been previously performed using this apparatus to examine the influence of gas temperature on the laser kinetics.[11] Those measurements showed that the gain decreases monotonically as the gas temperature increases. Comparison between measured and calculated gain indicated that the gas temperature dependent performance of the high pressure atomic xenon laser is consistent with reduced excitation of the upper laser levels due to a decreased rate of

dimer formation and dissociative recombination, and collisional mixing of the upper and lower energy level manifolds.[11]

In addition to measurements of the gain, Konak et al.[16] and Magda[17] demonstrated that the laser output power of the transitions at 1.73, 2.03 and 2.65 μm in atomic xenon are strongly temperature dependent. Using the $^3He(n,p)^3H$ pumping reaction, with a combined fission-fragment energy of 0.75 MeV, Konak et al. measured a decrease in laser output with increasing gas temperature at both 2.03 and 2.65 μm.[16] The gas mixture was ^3He/Ar/Xe (0.495/0.495/0/0.01) at a constant density (1 atmosphere at 293 K) while the laser cavity had an output coupling of 6 percent at 2.03 μm and 9 percent at 2.65 μm. The pump power was approximately 30 W/cm^3. The 2.03 μm laser energy was constant for gas temperatures between 293 K and 450 K and decreased to zero at 623 K. In contrast, the 2.65 μm laser energy terminated at 523 K. Magda showed that for ^{235}U fission-fragment pumping, the 1.73 and 2.03 μm laser output energies monotonically decreased to zero at a gas temperature of approximately 573 K.[17] The gas mixture was He/Ar/Xe (49.825/49.825/0.25) at a total pressure of 840 Torr and energy deposition of 110 J/L. Unfortunately, an energy loading of this magnitude produces transient gas temperature increases on the order of 200 K and makes separating kinetic effects difficult.

In strong contrast to the experiments discussed above, Batyrbekov and coworkers demonstrated 1.73 μm atomic xenon laser output that was insensitive to gas temperatures of up to 900 K.[18] These experiments used an electric-discharge pumped laser in which the gas mixture was ionized by radiation from a continuously operating nuclear reactor. They showed that the output energy in a $^4He/^3He$/Ar/Xe (50/50/50/1, 1.5 atm.) gas mixture was independent of gas

temperature for several neutron flux densities. This result is somewhat unexpected and indicates that additional kinetic processes may strongly influence the atomic xenon laser system. Possible additional mechanisms include modified electron temperature or density due to the influence of the external electric field. Whatever the mechanism, it is clear that our theoretical understanding of the important kinetic processes is incomplete.

In addition to design of the system to reduce the gas temperature, the effects of gas temperature can be reduced by adding buffer gases to Ar/Xe. Gas engineering, or the addition of selected buffer gases has long been used in gas laser physics to modify the electron energy distribution or increase the heat capacity of a gas mixture. For example, Basov and coworkers showed that neon addition can enhance the output energy of several laser systems without decreasing efficiency for neon/helium ratios less than 1/1 in He/Ar, He/Kr and He/Xe gas mixtures.[35] For the case of helium or neon addition to Ar/Xe mixtures, several points must be remembered. Codes suggest that one of the dominant production mechanisms for the upper laser level is the recombination of $ArXe^+$. If too much argon is removed, the $ArXe^+$ formation rate decreases. Since recombination of $HeXe^+$ and $NeXe^+$ are not expected to be a major contribution due to their weak binding[36] and the population of Xe_2^+ may be low since it is a minor gas constituent, it appears that there should be some minimum amount of argon required in the gas mixture.

The addition of helium or neon can also affect the quenching of the energy levels in the xenon laser manifold.[37-40] The net result of diluent addition may be a decrease or increase in gain or saturation intensity for the many transitions in the xenon manifold. In a broadband optical

cavity this is manifested in the observation of a shift in the dominant output wavelength. For example, Alford showed that argon quenches the lower laser level of the 1.73 μm transition an order of magnitude faster than the lower level of the 2.03 μm transition.[37] As a result, Ar/Xe mixtures lase at 1.73 μm in a broad band optical cavity. However, helium has just the opposite effect. The helium quenching rate for the lower level of the 2.03 μm transition is larger than the quenching rate for the lower level of the 1.73 μm transition. As helium was added to Ar/Xe gas mixture, the dominant output wavelength in a broadband optical cavity shifted from 1.73 μm to 2.03 μm. Neon has a small quenching rate for both the 1.73 and 2.03 μm transitions and did not change the output wavelength from 1.73 μm in Ne/Ar/Xe gas mixtures. 2.65 μm laser output was not observed, probably because this experiment used quartz Brewster angle windows (quartz has a strong absorption at 2.6 μm due to a OH absorption band). For an oscillator forced to operate at a given wavelength due to high mirror reflectivities at the desired wavelength and low reflectivities at the all other wavelengths, the addition of diluent may not be a problem. For an amplifier, an increase in gain at an undesired wavelength could result in amplified spontaneous emission reducing the gain on the desired transition. As a result of previous studies, neon and helium appears to be candidates for addition to Ar/Xe gas mixtures to reduce the effects of gas heating.

The quenching rates for the lower laser level of the 2.65 μm transition have been measured by a number of groups.[35,37-40] Quenching rates for the $6p[1/2]_0$ state, the lower level of the 2.65 μm laser are relatively high for Helium and Argon. This would partially explain why the 2.65 μm laser usually appears in broadband laser cavities. The quenching rate of the $6p[1/2]_0$ state is relatively low for neon; the quenching rate of neon is also low for the rest of the 6p

manifold. As a result, neon can be added to gas mixtures with a minimum effect on the kinetics. However, as Basov et al.[35] and Hebner et al.[13-15,41] showed, the addition of neon improves the stopping power of the gas mixture and increases the energy deposition. The net effect is an increase in output energy without decreasing laser efficiency (over a limited range of neon addition).

Reducing the gas temperature also reduces the hot gas induced index gradients in the laser cell. Side pumped lasers can have strong density and index gradients in the laser cell as the result of the excitation geometry which can give rise to a time dependent intracavity lens.[42-45] Under some pump and gas conditions, the heat induced lensing in the gain region can cause the cavity to go unstable. Since helium and neon reduce the absolute magnitude of the gas temperature rise, the index change in gas mixtures containing helium and neon is also reduced.

4.0 Review of electron beam pumped data

This section will review a fraction of the available literature on electron beam pumping of atomic xenon with an emphasis on the 2.65 μm transition. Information about the other atomic xenon transitions that have an impact on understanding the laser kinetics, such a pressure broadening rates, will be discussed. In addition, experimental data on the 2.65 μm laser operating at the same pump rate as nuclear excitation will be examined in detail to derive laser efficiencies. Finally, work demonstrating a continuous wave laser operation at 2.65 μm will be reviewed.

4.1 Laser characteristics at high pump rates (P > 100 W/cm^3)

Electron beam pumping of atomic xenon has been investigated by a large number of research groups.[33,35,46-65] As with nuclear pumping, the majority of these investigations focused on the 1.73 μm transition. However, some of the studies reported on the characteristics of the 2.65 μm transition. It is the conclusions from those works which will be review in this section. Since most of the electron beam pumped work was at pump rates far above the range of interest, the results can only serve as an aid to understanding the important kinetics of the xenon system.

Suda and coworkers[59,60] measured the small signal gain and saturation intensity in Ar/Xe gas mixtures. At a pump rate of 42 kW/cm^3, the gain was 6.4, 6.0 and 8.2 %/cm for the 1.73, 2.03 and 2.63 μm transitions respectively. The gain for the 2.65 μm transition was between 100 and 200 %/cm. However, the saturation intensity was between 0.1 and 0.2 kW/cm^2 for the 2.65 μm line; the saturation intensity for the 1.73, 2.03 and 2.63 μm lines was 17, 6.5 and 1.9 kW/cm^2 respectively. Thus the gain for the 2.65 μm line is relatively high, which explains the fact that it always appears in experiments with broad band cavities. In addition to measurements of the gain

and saturation intensity, they also examined the effects of gain competition on the spectrum of the laser output. They note that although the 2.65 μm transition starts lasing before the 1.73 μm line, the output at 2.65 μm is subsequently lower or terminated when the 1.73 μm transition begins to lase strongly. At the end of the pump pulse, the 1.73 μm lines terminates and the 2.65 μm line resumes output. Since the 1.73, 2.03 and 2.65 μm transitions all share a common upper laser level, it is not unreasonable to expect that there will be some competition for the population of the upper laser level.

While it is illustrative to examine the temporal history of the laser lines in a broad band cavity to understand the kinetics of the laser population, it does not rule out high output power on relatively weak lines. In reactor pumping experiments, we have demonstrated that it is relatively easy to use narrow band dielectric optics to suppress laser oscillation on strong laser lines and allow weaker lines to use the population in the upper laser level.[14,15,41,66,67] For example, in He/Ar/Xe gas mixtures, the dominate laser line is usually the 2.03 μm transition. However, we have demonstrated highly efficient laser output at 1.73 μm using narrow band dielectric mirrors to quench the laser output of the 2.03 μm line.[14,15] This same technique could be applied to the 2.65 μm transition to funnel the upper state population into the 2.65 μm laser.

Brannon et al.[62] and Suda et al.[60] have measured the pressure broadening rate for several of the atomic xenon transitions using electron beam excitation. Brannon used a novel technique based upon the Zeeman effect to measure the gain bandwidth of the 1.73 μm transition.[62] The Zeeman effect originated from the magnetic field used to guide the electron beam into the laser chamber. In general, the results of Brannon are in good agreement with the results obtained by Vetter et al. (discharge excitation)[68,69] and Hebner et al. (fission fragment excitation).[70] The

results of Suda are significantly higher than the results of Brannon. Pressure broadening rates were dependent on the gas mixture and laser transition. However, all of the values are between 8 and 25 MHz / Torr.

Patterson et al. examined the output of electron beam pumped xenon laser performance using two different electron beam machines.[33,61] The first utilized a 1 MeV electron beam guided into the laser cell and along the laser axis by an external magnetic field.[61] This system was capable of pump rates between 40 and 1000 W/cm^3. The variation in laser power at 1.73 and 2.65 μm was examined as a function of laser gas conditions and pump rate. They noted the laser pulse width was a function of the gas temperature (energy loading of the gas) and that the gas mixture could be modified to reduce the effects of gas temperature on the laser width and efficiency. Similar results were also obtained for the 1.73 and 2.03 μm laser using fission fragment pumping.

4.2 Laser characteristics at low pump rates (P < 100 W/cm^3)

The second system utilized by Patterson and coworkers was an electron beam machine designed to closely simulate nuclear pumped conditions (KITE).[33] The electron beam was capable of supplying pump rates in the approximate range of 5 to 100 W/cm^3 with pulse widths 5 to 55 milliseconds. Two sets of cavity optics were used for these experiments. The first was a set of narrow band dielectric mirrors used to determine the laser gain and saturation intensity at 1.73 μm. The gas mixture was Ar/Xe at a total pressure of 840 Torr, Xe fraction of 0.5 percent, and pump rates of 12, 22 and 42 W/cm^3. The measured values of gain, 0.64 , 0.64 and 0.91 %/cm, and saturation intensity, 61, 160, 381 W/cm^2 for pump rates of 12, 22 and 42 W/cm^3,

respectively, are in good agreement with reactor pumped data by Hebner and Hays[14] and Perkins et al.[47]

The second set of cavity optics was broadband to examine the effects of line competition (broad band optics were discussed in section 2.2). Since the work by Patterson et al. is the only study of the 2.65 μm transition that uses electron beam excitation for pump conditions that simulate reactor pumping, it will be examined in detail.[33] For the purposes of this review, the parameter of interest is the efficiency of the 2.65 μm transition as a function of gas mixture, pressure and pump power. Patterson et al. report the total laser output (in Watts) in a broadband laser cavity and the relative fraction of 1.73, 2.03 and 2.65 μm laser output for pump powers between 5 and 60 W/cm^3. This information can be converted to efficiency if one knows the pump volume and assumes that the laser output is uniform over the pump aperture. Based upon conversations with E. L. Patterson, this experiment used a 3 cm diameter aperture at the output of the laser cavity.[71] As a result, the laser pump volume is 7 cm^2 x 100 cm = 700 cm^3.

The results of converting the data of Patterson et al. to laser efficiency is shown in Table 3.[33] The efficiency is approximately 0.1 to 0.5 percent; less than the nuclear pumped values reported by Melnikov and Sinyanskii (Table 2),[20] but consistent with the values reported by Magda.[17]. Since the program at Sandia National Laboratories was focused on the 1.73 μm transition, no attempt was made to optimize the 2.65 μm laser output. Some of the data from Patterson, in particular the data for He/Ar/Xe gas mixtures, indicates that the efficiency increased as the pump rate was decreased. As a result, it appears that it may be possible to improve the efficiency of the 2.65 μm laser.

Table 3. Electron beam pumped efficiency at 2.65 μm as a function of pump power, gas mixture, total pressure and buffer gas ratio.[33]

Ar Xe, 254 Torr, 1:0.005	
Pump power (W)	Efficiency (%)
5.0	0.28
15.0	0.31
35.0	0.21

Ar Xe, 507 Torr, 1:0.005	
Pump power (W)	Efficiency (%)
5.0	0.22
15.0	0.19
60.0	0.32

Ar Xe, 760 Torr, 1:0.005	
Pump power (W)	Efficiency (%)
5.0	0.18
15.0	0.29
60.0	0.47

Ne Ar Xe, 760 Torr, .66:.33:.005	
Pump power (W)	Efficiency (%)
5.0	0.18
15.0	0.34
55.0	0.29

He Ar Xe, 760 Torr, .66:.33:.005	
Pump power (W)	Efficiency (%)
5.0	0.33
15.0	0.18
28.0	0.10

Perkins et al. also investigated the pumping of atomic xenon using a long pulse electron beam machine.[47] They measured values for the 1.73 μm atomic xenon transition gain, saturation intensity and efficiency that were in good agreement with both Patterson[33] and Hebner.[13,14]

4.3 CW 2.65 μm laser

In addition to operating in the pulse mode, the 2.65 μm transition has been observed to lase cw when pumped by a transverse radio frequency discharge. Udalov et al. reported unoptimized output powers of 80 - 100 mW at 2.65 μm at a pressure of 85 Torr in He/Ar/Xe gas mixtures.[72] The laser was pumped at 150 W using an excitation frequency of 121 MHz and laser output was observed at 2.03, 2.63, 2.65, 3.37 and 3.51 μm.

Hebner has also observed quasi-cw (20 ms pulse length) laser action at 2.03 μm using microwave excitation of He/Xe gas mixtures.[73] Unoptimized laser powers of approximately 1 mW were observed for microwave (2.45 GHz) pump powers of 300 W. It was noted that the laser output was very sensitive to gas heating. Laser output at 2.65 μm was not investigated.

5.0 Conclusions

The characteristics of the 2.65 μm atomic xenon laser transition have been reviewed. Data from both electron beam and nuclear pumping was examined. A laser efficiency between 0.1 and 2 percent has been reported, although there is some uncertainty in the values above 1 percent. Electron beam pumped atomic xenon studies imply that under certain conditions, the efficiency of the 2.65 μm transition may improve at lower pump rates. Since no studies have focused on this transition exclusively, it is possible that improvements in this efficiency are possible.

References

1. A. M. Voinov, L. E. Dovbysh, V. N. Krivonosov, S. P. Melnikov, A. T. Kazakevich, I. V. Podmoshenskii, and A. A. Sinyanskii,Sov. Tech. Phys. Lett. 54, 171(1979).
2. J. R. Felty, R. J. Lipinski, D. A. McArthur and P. S. Pickard, Proc. SPIE, 2121, 2 (1994).
3. G. A. Hebner, Proc. SPIE 2121, 10 (1994).
4. A. M. Voinov, Laser Particle Beams 11, 635 (1993).
5. P. P. Dyachenko, Laser Particle Beams 11, 619 (1993).
6. G. H. Miley, Laser Particle Beams 11, 575 (1993).
7. A. I. Miskevich, Laser Physics 1, 445 (1991).
8. R. T. Schneider and F. Hohl in *Advances in Nuclear Science and Technology,* vol. 16 edited by J. Lewins and M. Becker, Plenum Press, New York, 1984, pgs. 123-288.
9. W. J. Alford and G. N. Hays, J. Appl. Phys. 65, 3760 (1989).
10. W. J. Alford, G. N. Hays, M. Ohwa and M. J. Kushner, J. Appl. Phys. 69, 1843 (1991).
11. G. A. Hebner, J. W. Shon and M. J. Kushner, Appl. Phys. Lett. 63, 2872 (1993).
12. G. A. Hebner and G. N. Hays, J. Appl. Phys. 71, 1610 (1992).
13. G. A. Hebner and G. N. Hays, J. Appl. Phys. 74, 3673 (1993).
14. G. A. Hebner and G. N. Hays, J. Appl. Phys. 73, 3614 (1993).
15. G. A. Hebner and G. N. Hays, J. Appl. Phys. 73, 3627 (1993).
16. A. I. Konak, S. P. Melnikov, V. V. Porkaev and A. A. Sinyanskii, Lasers Particle Beams 11, 663 (1993).
17. E. P. Magda, Lasers Particle Beams 11, 469 (1993).

18. G. A. Batyrbekov, E. G. Batyrbekov, V. A. Danilychev, A. B Tleuzhanov and M. U. Khasenov, Sov. J. Quantum Electron. 19, 1393 (1990).

19. A. M. Voinov, A. A. Sinyanskii, A. G. Vasilenko, O. A. Golubeva. L. E. Dovbysh, V. V. Ivanov, M. I. Kuvshinov, B. V. Lazhintsev, A. E. Lakhtikov, S. P. Melnikov, A. B. Modenov. V. A. Nor-Arevyan, A. M. Pichugin. A. N. Pokalo, V. V. Porkhaev, Ya. A. Pospelov, A. V. Sinitsyn, I. G. Smirnov, S. L. Turutin and M. V. Khlestkov, Second Specialist International Conference on Physics of Nuclear Induced Plasmas and Problems of Nuclear Pumped Lasers, September 26-30, 1994, Arzamas-16, Russia.

20. S. P. Melnikov and A. A. Sinyanskii, Lasers particle beams 11, 645 (1993).

21. R. J. DeYoung, N. W. Jalufka and F. Hohl, Appl. Phys. Lett. 30, 19 (1977).

22. R. J. DeYoung, Y. J. Shiu and M. D. Williams, Appl. Phys. Lett. 37, 679 (1980).

23. A. M. Voinov, L. E. Dovbysh, V. M. Krivonosov, S. P. Melnikov, I. V. Podmoshenskii and A. A. Sinyanskii, Sov. Tech. Phys. Lett. 7,437 (1981).

24. A. M. Voinov, A. S. Koshelev, S. P. Melnikov and A. A. Sinyanskii, Sov. Tech. Phys. Lett. 16, 517 (1990).

25. P. J. Brannon, E. L. Patterson and G. E. Samlin, Sandia report, SAND90-0202, Sandia National Laboratories, Albuquerque NM 87185.

26. J. W. Shon, M. J. Kushner, G. A. Hebner and G. N. Hays, J. Appl. Phys. 73, 2686 (1993).

27. M. Ohwa, T. J. Moratz and M. J. Kushner, J. Appl. Phys. 66, 5131 (1989).

28. J. W. Shon and M. J. Kushner, J. Appl. Phys. 75, 1883 (1994).

29. T. J. Moratz, T. D. Saunders and M. J. Kushner, J. Appl. Phys.64, 3799 (1988).

30. M. J. Berger and S. M. Seltzer, Studies in Penetration of Charged Particle in Matter (National Academy of Sciences - National Research Council, Washington D.C., 1964) pgs. 205 - 268.

31. M. S. Moore and L. G. Miller, Phys. Rev. 157, 1049 (1967).

32. T. J. Moratz and M. J. Kushner, J. Appl. Phys. 63, 1796 (1988).

33. E. L. Patterson and G. E. Samlin, J. Appl. Phys. 2582 (1994).

34. A. P. Hickman, D. L. Huestis and R. P. Saxon, J. Chem. Phys. 98, 5419(1993).

35. N. G. Basov, V. V. Baranov, V. A. Danilychev, A. Yu. Dudin, D. A. Zayarnyi, L. V. Semenova, N. N. Ustinovskii, I. V. Kholin and A. Yu. Chugunov, Sov. J. Quantum Electron 16, 320 (1986).

36. J. S. Cohen and R. T. Pack, J. Chem. Phys. 61, 2372 (1974).

37. W. J. Alford, IEEE J. Quantum Electron. QE-26, 1633 (1990).

38. W. J. Alford, J. Chem. Phys. 96, 4330 (1992).

39. J. Xu and D. W. Setser, J. Chem. Phys. 92, 4191 (1990).

40. J. Xu and D. W. Setser, J. Chem. Phys. 94, 4243 (1991).

41. G. A. Hebner, IEEE J. Quantum Electron. QE-29, 2356 (1993).

42. J. R. Torczynski and D. R. Neal, Nuclear Science and Engineering, 113, 189 (1993).

43. D. R. Neal, J. R. Torczynski and W. C. Sweatt, Optical Eng. 29, 1404 (1990).

44. D. R. Neal, W. C. Sweatt and J. R. Torczynski, Current Developments in Optical Engineering (Society of Photo-Optical Instrumation Engineers, Bellingham WA, 1989), Vol. 965, pg 130.

45. W. A. Neuman and J. R. Fincke, J. Appl. Phys. 69, 6789 (1991).

46. S. A. Lawton, J. B. Richards, L. A. Newman, L. Specht and T. A. DeTemple, J. Appl. Phys. 50, 3888 (1979).

47. T. Perkins, X. Chen and J. Jacob, Conference on Lasers and Electro-optics, May 1991, Baltamore MA.

48. V. V. Baranov, V. A. Danilychev, A. Yu. Dudin, D. A. Zayarnyi, A. V. Romanov, N. N. Ustinovskii, I. V. Kholin and A. Yu. Chugunov, Sov. Phys. Tech. Phys. 33, 1328 (1989).

49. J. E. Tucker and B. L. Wexler, IEEE J. Quantum Electron. QE-26, 1647 (1990).

50. N. B. Basov, A. Yu. Chugunov, V. A. Danilychev, I. V. Kholin and M. N. Ustinovsky, IEEE J. Quantum Electron. QE-19, 126 (1983).

51. N. G. Basov, V. A. Danilychev, A. Yu. Dudin, D. A. Zayarnyi, N. N. Ustinovski, I. V. Kholin, and A. Yu. Chugunov, Sov. J. Quantum Electron. 14, 1158 (1984).

52. N. G. Basov, V. V. Baranov, A. Y. Chugunov, V. A. Danilychev, A. Y. Dudin, I. V. Kholin, N. N. Usinovskii and D. A. Zayarnyi, IEEE J. Quantum Electron. QE-21, 1756 (1985).

53. N. G. Basov, V. V. Baranov, V. A. Danilychev, A. Yu. Dudin, D. A. Zayarnyi, L. V. Semenova, N. N. Ustinovskii, I. V. Kholin and A. Yu. Chugunov, Sov. J. Quantum Electron 16, 316 (1986).

54. A. R. Sorokin, Sov. Phys. Tech. Phys. 24, 932 (1979). 11. A. R. Sorokin, Sov. J. Quantum Electron. 13, 165 (1983).

55. A. R. Sorokin, Sov. J. Quantum Electron. 13, 165 (1983).

56. V. O. Petukhov, S. Ya. Tochitskii and V. V. Curakov, Sov. J. Quantum Electron. 18, 318 (1988).

57. P. J. M. Peters, Mei Qi-Chu and W. J. Witteman, Appl. Phys. B 47, 187 (1988).

58. B. M. Berkeliev, V. A. Dolgikh, I. G. Rudoi and A. M. Soroka, Sov. J. Quantum Electron. 20, 1439 (1990).

59. Akira Suda, Bernard L. Wexler, Barry J. Feldman and Kevin J. Riley, Appl. Phys. Lett. 54, 1305 (1989).

60. Akira Suda, Bernard L. Wexler, Kevin J. Riley and Barry J. Feldman,IEEE J. Quantum Electron. QE-26, 911 (1990).

61. E. L. Patterson, G. E. Samlin, P. J. Brannon, M. J. Hurst, IEEE J. Quantum Electron. QE-26, 1661 (1990).

62. Paul J. Brannon, R. W. Morris and Edward L. Patterson, IEEE J. Quantum Electron. QE-26, 1653 (1990).

63. C. R. Mansfield, P. F. Bird, J. F. Davis, T. F. Wimett and H. H. Helmick, Appl. Phys. Lett. 30, 640 (1977).

64. I. Derzhiev, A. G. Zhidkov, O. V. Sereda, V. S. Skakun, V. F. Tarasenko, A. V. Fedenev and S. I. Yakovlenko, Sov. J. Quantum Electron. 20, 902 (1990).

65. L. N. Litzenberger, D. W. Trainor, and M. W. McGeoch, IEEE JQE-26, 1668 (1990).

66. G. A. Hebner and G. N. Hays, Appl. Phys. Lett. 57, 2175 (1990).

67. G. A. Hebner, J. Appl. Phys. 74, 2203 (1993).

68. R. Vetter and D. Reymann, J. Phys. B 7, 323 (1974).

69. O. Vallee, E. Marie, N. Tran Minh and R. Vetter, Phys. Rev. A 24, 1391 (1981).

70. G. A. Hebner and G. N. Hays, Appl. Phys. Lett. 59, 537 (1991).

71. E. L. Patterson, private communication.

72. Y. B. Udalov, P. J. M. Peters, M. B. Heeman-Illieva, F. H. J. Ernst, V. N. Ochkin and W. J. Wittman, Appl. Phys. Lett. 721 (1993).

73. G. A. Hebner, 41 st Gaseous Electronics Conference, Urbana IL, 1990.

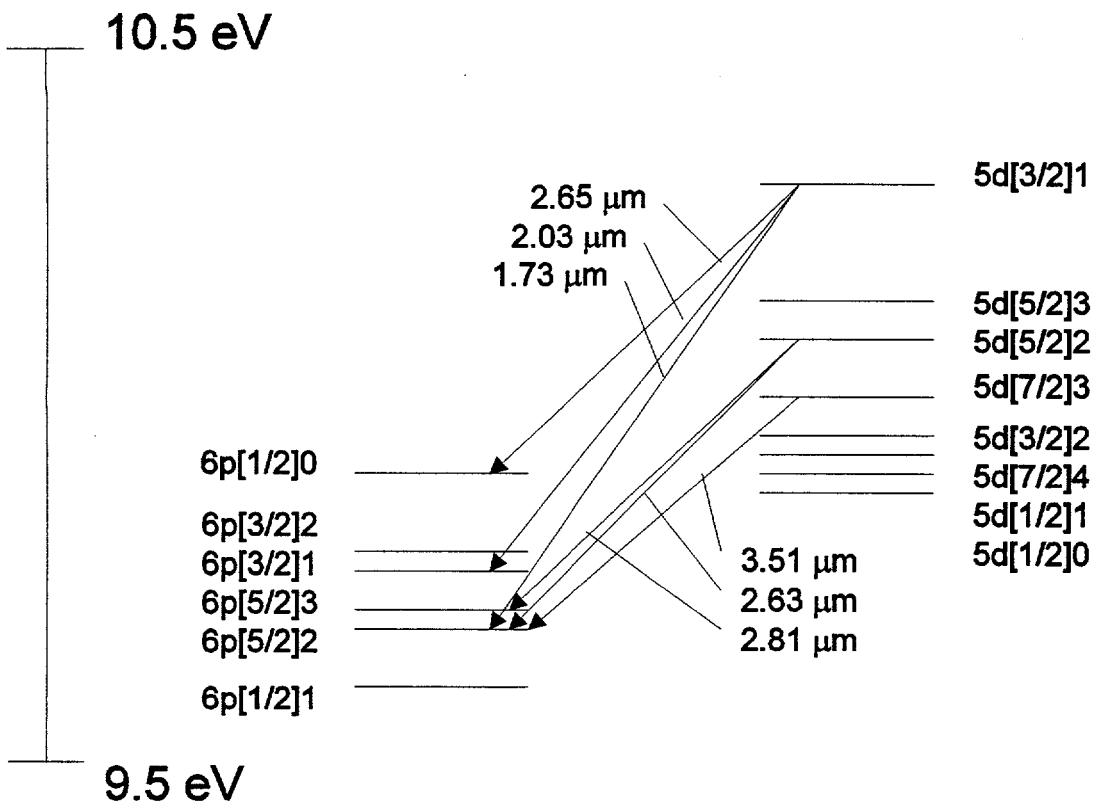

Fig. 1 Partial energy level diagram of atomic xenon

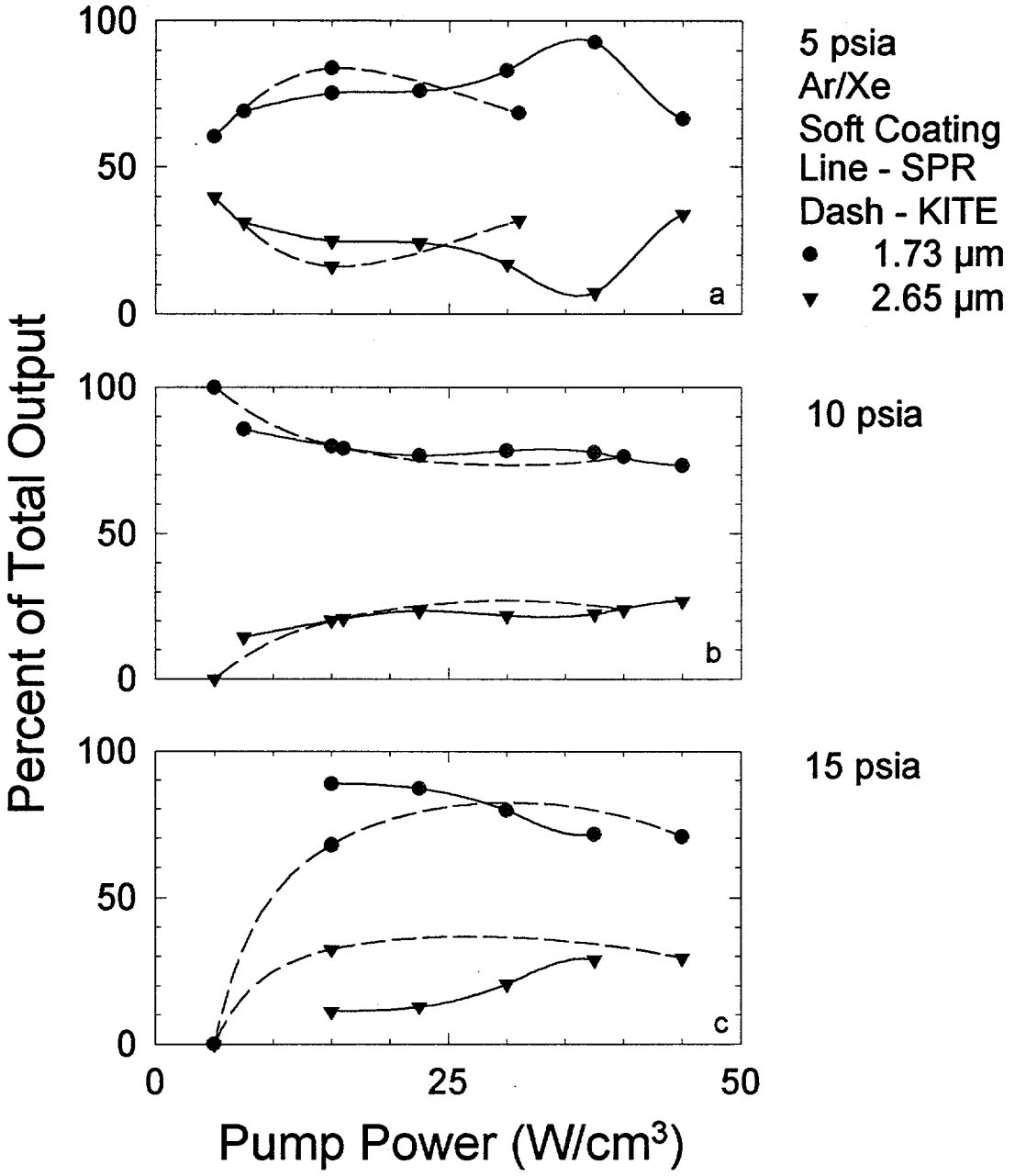

Fig. 2 Comparison of the relative output at 1.73 (●) and 2.65 (▼)mm using electron beam (KITE, dashed line) and fission fragment (SPR-III, solid line) pumping. The gas mixture was Ar/Xe with a 0.5 percent xenon fraction in 5 (a), 10 (b) and 15 (c) psia of argon. The output coupler labeled "soft coating" was used for both experiments.

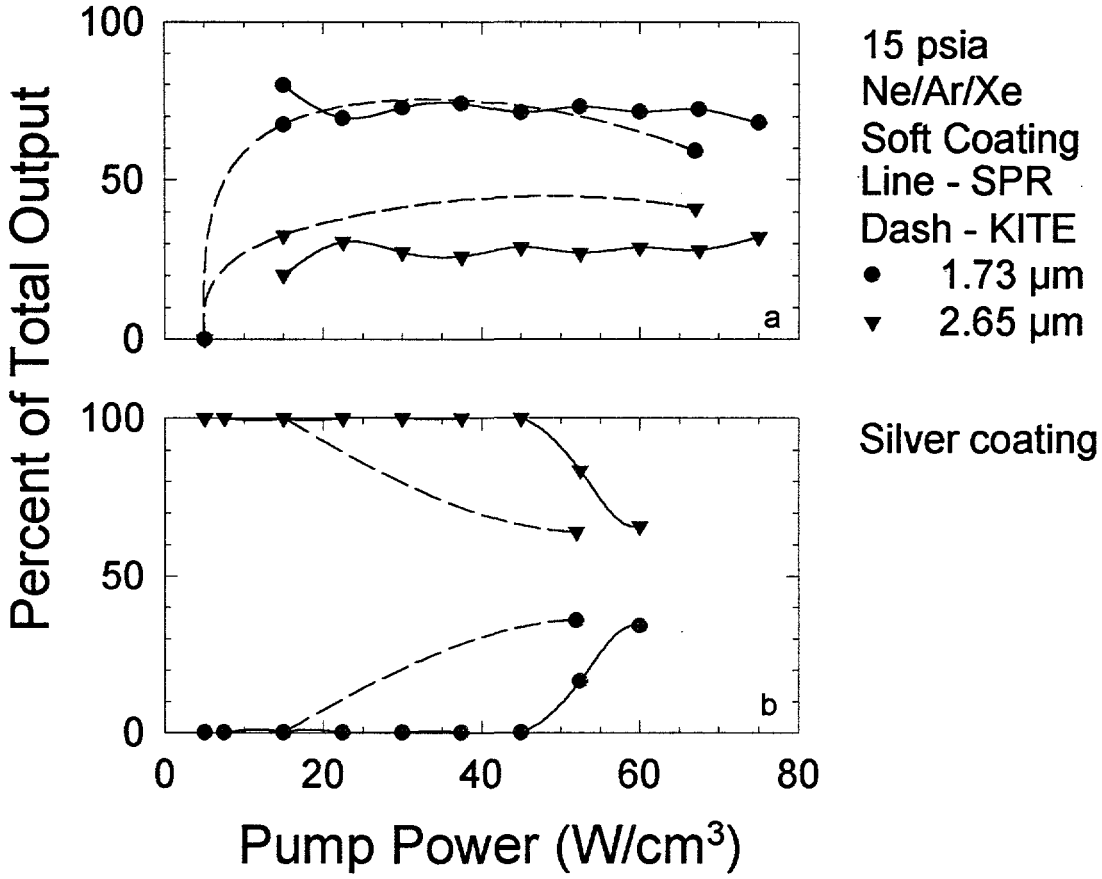

Fig. 3 Comparison of the relative output at 1.73 (●) and 2.65 (▼)mm using electron beam (KITE, dashed line) and fission fragment (SPR-III, solid line) pumping. The gas mixture was Ne/Ar/Xe (0.66/0.33/0.005) at 15 psia. The output coupler was the soft coating (a); and the silver coating (b).

Distribution:

1	MS1423	G. N. Hays, 1128
5	1423	G. A. Hebner, 1128
1	1423	P. J. Brannon, 1128
1	1145	P. S. Pickard, 6514
10	1145	R. J. Lipinski, 6514
1	9018	Central Technical Files, 8523-2
5	0899	Technical Library, 13414
1	0619	Print Media, 12615
2	0100	Document Processing, 7613-2 For DOE.OSTI